

Figure S1. Typical surface features reflectance of Lake Taihu from MODIS, OLI, MSI, and OLCI images.

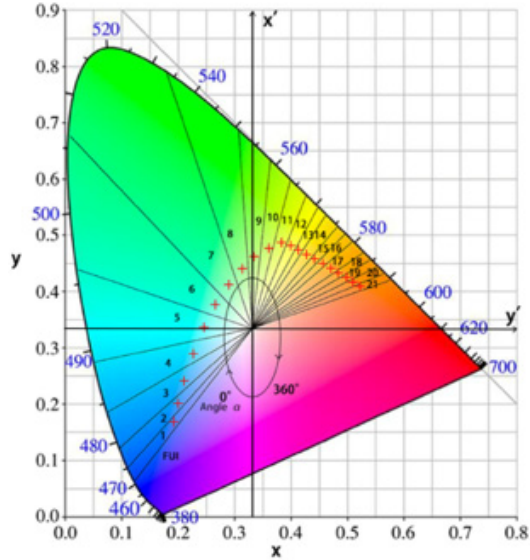


Figure S2. CIE-xy chromaticity diagram and display of calculating hue angle α according to [101] and [80].

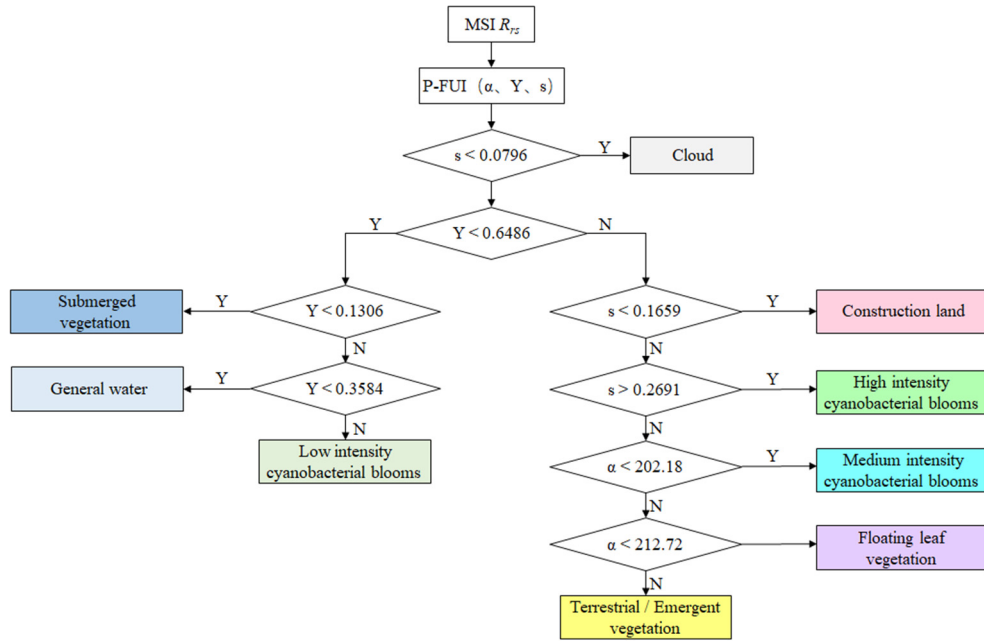


Figure S3. Flowchart of discriminating various land covers based on the P-FUI decision tree.

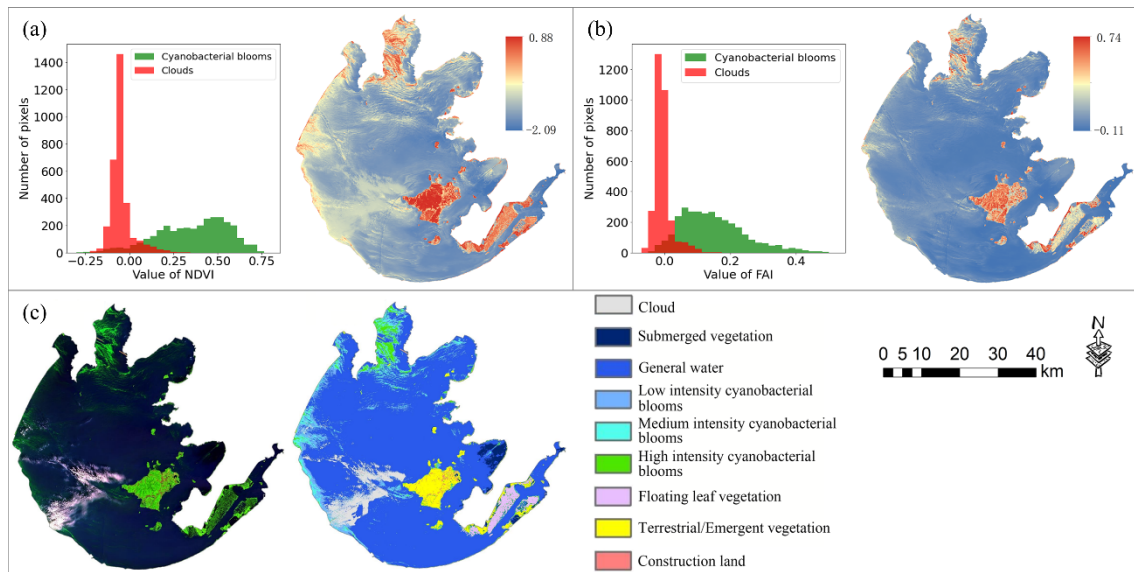


Figure S4. Comparison of different methods (P-FUI, NDVI, and FAI) to distinguish cyanobacterial blooms and clouds based on the OLI images (Aug. 21, 2019, Lake Taihu). (a) Histogram of NDVI covered by cyanobacterial blooms and clouds based on "ground truth", and the spatial distribution of NDVI in the lake. (b) Histogram of FAI covered by cyanobacterial blooms and clouds based on "ground truth", and the spatial distribution of NDVI in the lake. (c) The left is the false-color composite image, while the right is the identification result based on the P-FUI algorithm.

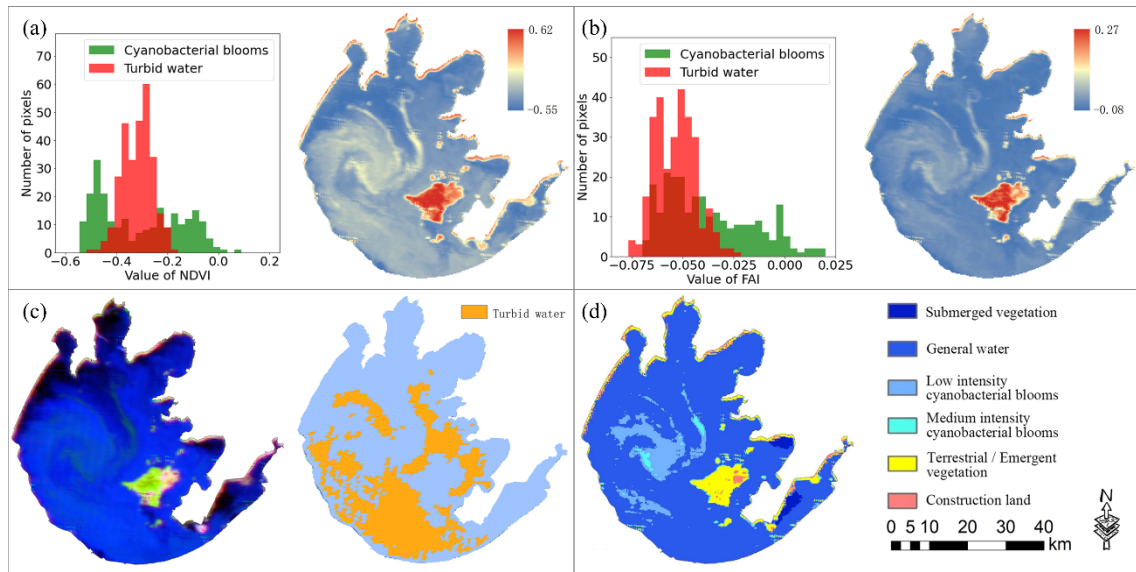


Figure S5. Comparison of different methods (P-FUI, NDVI, and FAI) to distinguish cyanobacterial blooms and turbid water based on the MODIS images (Feb. 18, 2020, Lake Taihu). (a) Histogram of NDVI covered by cyanobacterial blooms and turbid water based on "ground truth", and the spatial distribution of NDVI in the lake. (b) Histogram of FAI covered by cyanobacterial blooms and turbid water based on "ground truth", and the spatial distribution of NDVI in the lake. (c) The left is the false-color composite image (B7-B2-B1), while the right is the identification result of turbid water according to [25]. (d) P-FUI classification results.

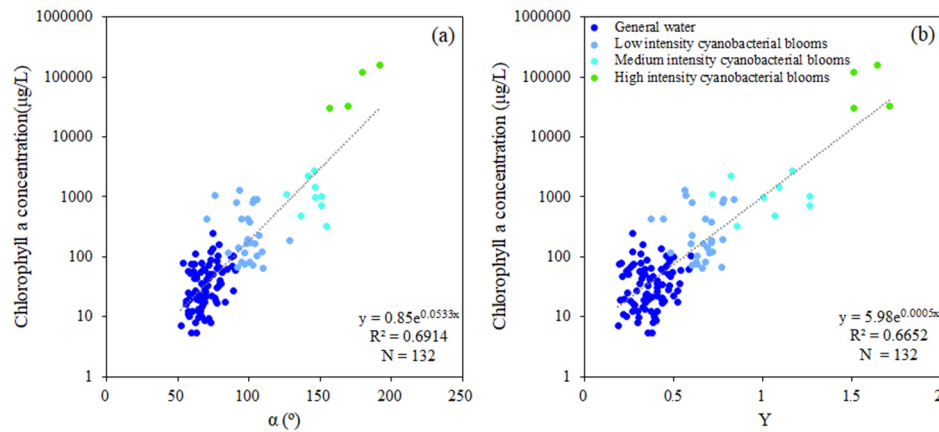


Figure S6. Relationships between the chlorophyll-a concentration and P-FUI parameters. (a) Relationships between the Chl-a concentration and hue angle α , (b) Relationships between the Chl-a concentration and brightness Y .

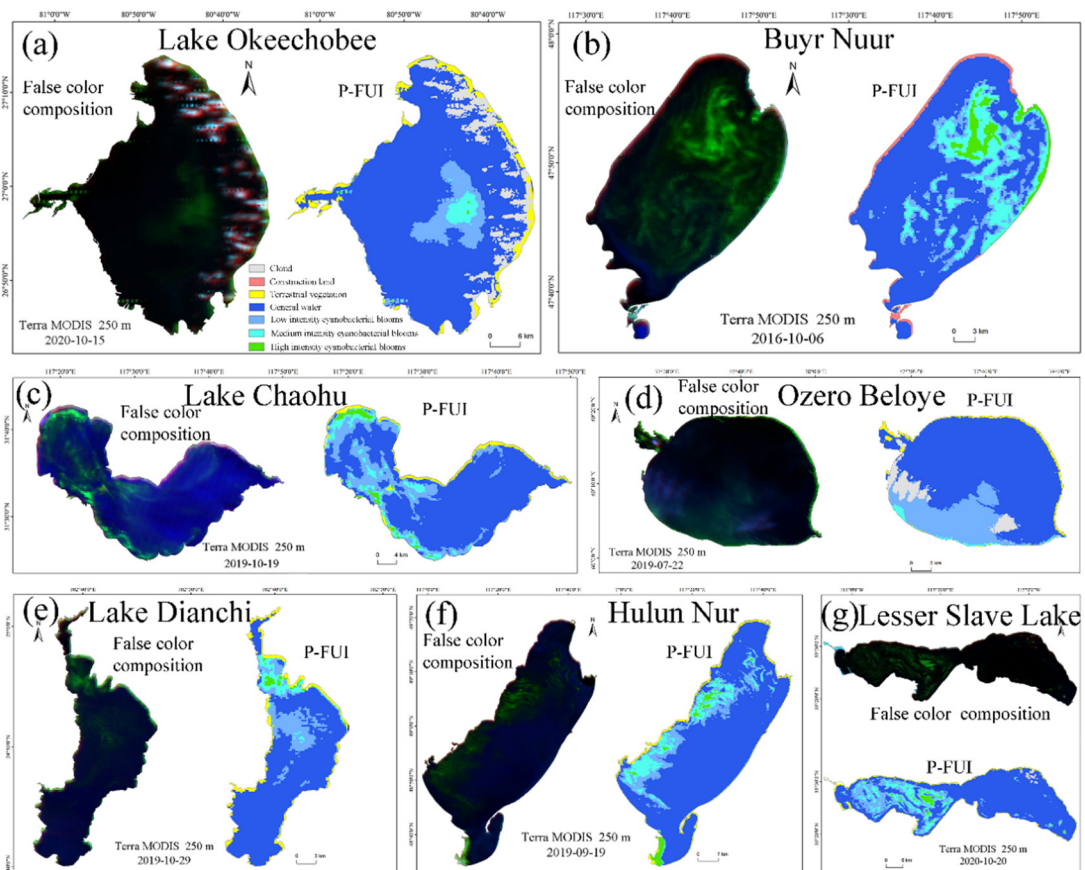


Figure S7. Cyanobacterial bloom identification results in other lakes using the PFUI algorithm based on MODIS images.

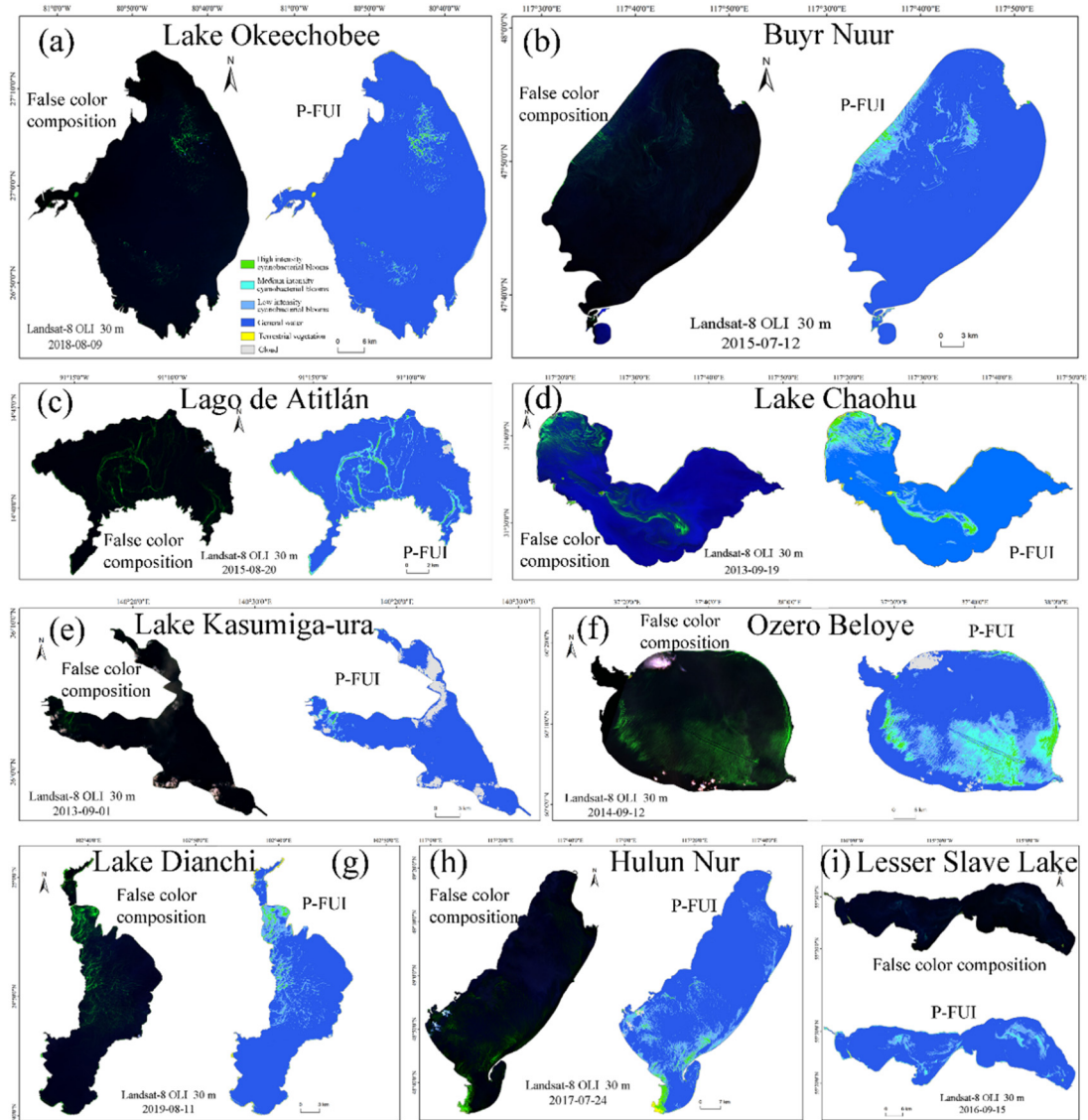


Figure S8. Cyanobacterial bloom identification results in other lakes using the PFUI algorithm based on OLI images.

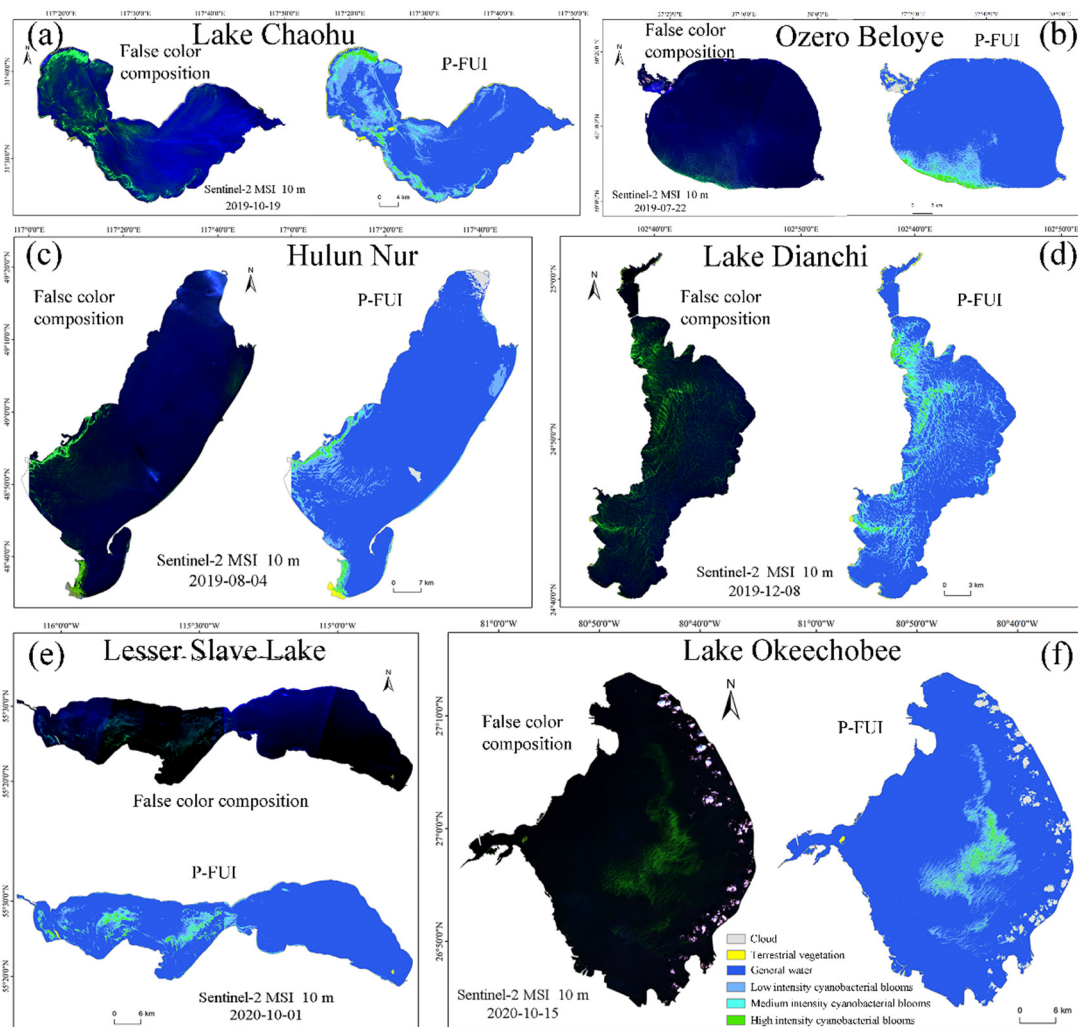


Figure S9. Cyanobacterial bloom identification results in other lakes using the PFUI algorithm based on MSI images.

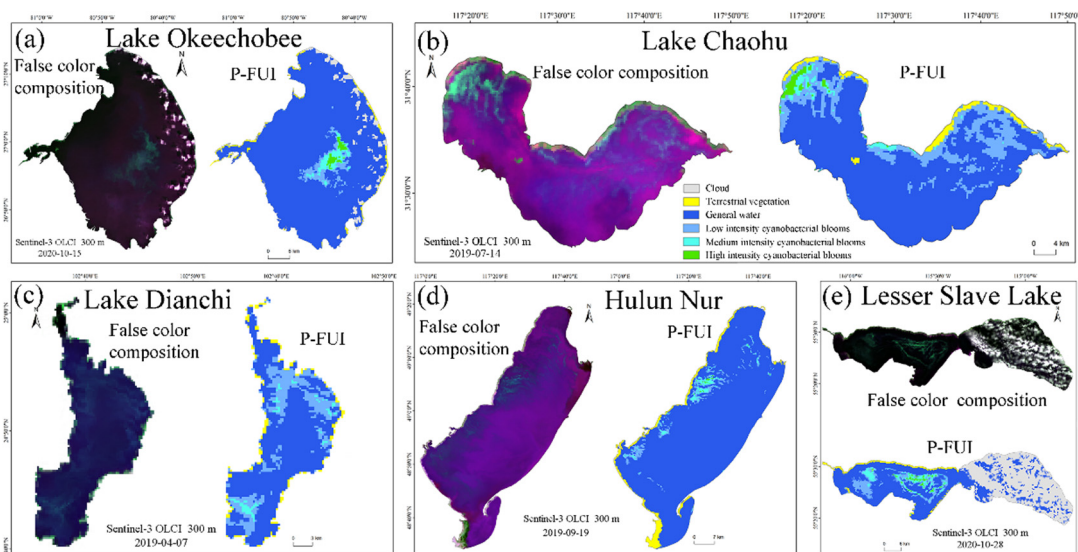


Figure S10. Cyanobacterial bloom identification results in other lakes using the PFUI algorithm based on OLCI images.

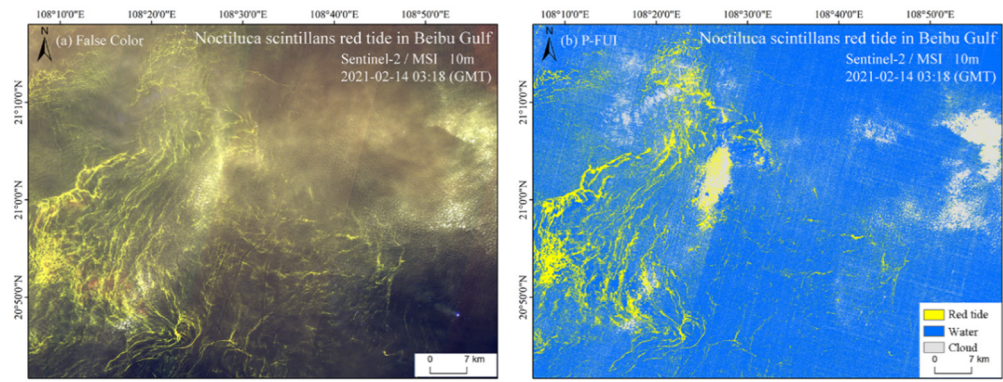


Figure S11. P-FUI extraction of *Noctiluca scintillans* red tide in Beibu Gulf based on MSI sensor.